Acta Microscopica Vol. 28, No.4, 2019, pp.733-744

Horizontal Bearing Capacity of Closely-spaced Row-piles Based on Microscopic Microstructure of Soft Soil

Runze Xue
State Key Laboratory of Hydraulic Engineering Simulation and Safety, Tianjin University, Tianjin 300000, China

Shean Bie*
State Key Laboratory of Hydraulic Engineering Simulation and Safety, Tianjin University, Tianjin 300000, China
**Corresponding author (E-mail: bieshean@tju.edu.cn)*

Abstract
The frame-fixed soldier pile structure (FSPS) is a new cofferdam structure of artificial island, with a notable feature of closely-spaced row-piles. Microstructure of soft soil has a significant effect on macroscopic physical quantities. The relationship between microstructure deformation characteristics of soft clay and shear strength index of soil was established by scanning electron microscope (SEM) test. Based on the subgrade reaction approach, a plane pole system finite element model (PPSFEM) was established to study displacement and internal force distribution along pile of FSPS under lateral load. The "load migrating" process was considered in the model that partial lateral load would transfer from rear pile to front pile via interior soil as interior soil reached the ultimate state. Study on how these factors affect the distribution of horizontal displacement and internal forces along pile has been performed through PPSFEM, including constraint form between frame structure and pile, m-values of subsoil and backfilling materials. The shear strength index of soil is significant affected by the microstructure. Parameter analysis indicates that the frame structure improves internal force distribution of pile foundation, that the feature of separated piles decreases the horizontal soil resistance of front pile, and that the articulated constraint form between pile and underpart of framework benefits to reduce the maximum bending moment of pile.

Key words: Soft Soil, Micro-Structure, Frame-Fixed Soldier Pile Structure, Double Row Pile Structure

1. Introduction

In the literature, structural form and engineering application of the frame-fixed soldier pile structure (FSPS) were introduced, and structural stability analysis was performed. The most notable feature of the FSPS is the closely-spaced row-piles, where the tiny pile spacing plays a key role in the horizontal bearing capacity. Considering that the macroscopic physical and mechanical properties of soil are affected to some extent by the state and change of micro-structure, the relationship between micro-parameters and macro-physical quantities of soft clay needs to be established [1-4]. There are many factors affecting the shear strength of soils. Based on the soil microstructure, the influencing factors of soil shearing strength were analyzed from the aspects of pore change and contact area, including structure, stress history, anisotropy, loading rate and consolidation.

This paper aims to study internal force calculation model of FSPS based on microscopic microstructure of soft soil. While the vertical bearing mechanism of FSPS is similar to that of the high-piled wharf structure, engineering researches pay close attention to horizontal displacement and internal force distribution along pile under lateral loads (such as lateral earth pressures). Existing calculation models of double sheet-pile wall structure (DSWS) are good references for strength analysis of FSPS [5]. A kind of plane model was adopted for DSWS with short row spacing of (2~5) d (d=diameter of pile) in strutted excavations. In this model, the tie rod and double-row piles were simplified as a rigid portal framework with tip elastic embedded in view of short row spacing, and filling was replaced by a number of springs connecting front and rear piles to avoid supposition of distribution coefficient of earth pressure between piles [6]. Another kind of plane model was for the wharf structure of double-rowed pipe piles with single anchor rod and relatively wide row spacing. By reinforcing the soil between double-row piles (denoted as "interior soil") and managing construction appropriately, the double-row piles and reinforced interior soil were treated as composite cantilever retaining wall with bottom fixed in the ground. Internal forces and lateral displacement of pipe piles were solved by elastic theory.

Although FSPS is based on traditional DSWS, specialized studies on internal forces is still needed by considering the influences of frame structure, row spacing and separated piles. Since piles are driven into soil through guiding beams and connected with framework by cast-in-situ concrete, the framework directly restricts deflection deformation of piles, and the size and stiffness of framework affect the shape and peak of pile displacement curve. Row spacing of FSPS (usually more than 10d) is much larger than that of DSWS in strutted excavations. Therefore, lateral earth pressure caused by interior soil gravity cannot be omitted. Group efficiency of each pile under lateral load is also related to row spacing. Since soft ground treatment is beneficial to

improving the bearing capacity but not economy, the calculation model proposed by Yu et al. (2004) is not suitable for FSPS filled with undisposed backfilling materials. Considering ideal elastic-plastic characteristics of interior soil, partial load transfers to front pile via interior soil under the ultimate state. With a large elevation difference between mud surfaces on piles' front and rear sides, the separated piles are subjected to the potential lateral soil movement (i.e. becoming so called "passive" piles), which gives rise to soil resistance of front pile decreasing [7-9].

Abundant researches have been carried out on behavior of laterally loaded pile and pile group in the way of numerical method [10, 11], experimental method and theoretical analysis such as subgrade reaction approach [12-15]. Considering the operability of structure design and calculation, a plane pole system finite element model (PPSFEM) based on subgrade reaction approach is adopted here to obtain the distribution of displacement and internal forces along soldier pile of FSPS. A test project is conducted to verify the feasibility of this model by comparing results gotten from FEM and field observations. Then PPSFEM is employed to study influences on pile internal forces of factors such as constraint form between pile and underpart of framework, m-values of subsoil and backfilling materials.

2. Microstructure Characteristics of Soft Soil

2.1. SEM Test

The microstructure of the soil refers to the shape, size, arrangement and combination, surface characteristics, structural connection and pore characteristics of the structural unit. At present, the commonly used instruments for studying the microstructure of soils include electron microscope, X-ray diffractometer, optical microscope, etc. The direct test method is used to analyze the scanned photographs to study the microstructure of the soil. In addition to direct observation methods, there are indirect methods, such as determining the pore structure, dielectric constant, conductance, sound waves, etc. of the soil to understand its microstructure characteristics.

The relationship between micro-parameters and macro-physical quantities of soft clay is established by statistical method based on the SEM test of soft clay. In this experiment, the cofferdam structure engineering of the 30,000-ton waterway project in Binzhou Port was studied. Firstly, the SEM microstructure analysis method was used to analyze the morphology and distribution of soft soil morphology and its parameters. The SEM test samples were prepared in a size about 10mm×10mm×15mm, using the liquid nitrogen freezing vacuum sublimation sample preparation technology to maintain the natural structure of the soil as much as possible. And select a representative soil sample fresh section, after the gold spray treatment, put the SEM electron microscope the test chamber was selected with appropriate magnification and representative field of view. The SEM image of the soft clay sample was taken with a Quanta650 scanning electron microscope. The magnifications were 500, 1000, 2000, 3000, 4000, and 6000. With the powerful graphics processing function in MATLAB, the SEM photos were processed by digital image. On this basis, the microstructure and shape of pores (particles), morphology and distribution were analyzed and calculated.

2.2. Structural Property of Soil

The SEM image of the soil sample according to the soft soil foundation treatment project is shown in Figure.1. The microstructure of the sample soft soil can be seen mainly in three types: floc structure, honeycomb structure, and clot structure.

(1) Floc structure: the clay content is large, the soil particles are surface-to-surface connection, the clay minerals are mainly kaolinite and montmorillonite; the clay particles are flocculent aggregates. The porosity is 40%~60%, distribution Uneven, the clay is a floc aggregate.

(2) Honeycomb structure: a porous, honeycomb-like structure formed; the soil particles are mainly surface-to-surface contact, and the clay particle size is 1~10μm. The content is more than 30%, the porosity is 40%~60%, and the structure is loose.

(3) Clot structure: aggregate mass composed of clay particles (particle size larger than 10μm), the powder particles are scattered on the surface of the mass or in the mass between the blocks, the content is less, and the connection function.

The clay content in the soft soil in marine area is generally high, and some of the powder particles, sand grains, mineral crystals and aggregates, and occasional biological debris are seen.

The undisturbed soil in the foundation has certain structural properties. Due to different geological history and environmental conditions, the structural strength of soil varies greatly. Taking clay as an example, the shear strength of soil is similar to that of over-consolidated soil before its structural failure, which mainly reflects the difference of cohesion of soil. From the aspect of pore size, it can be considered that the smaller the porosity, the larger the contact area of clay particles and the stronger the cohesive force. This is in sharp contrast with the point contact of non-cohesive soil. For non-cohesive soil, the contact is basically point contact, so the cohesive force is almost zero. Before the structural property of soil is not destroyed, the stronger the structural property of

soil is, the higher the shear strength of soil is. Because of the structure of undisturbed soils, the molar envelope obtained from tests of normally consolidated undisturbed soils often does not pass through the origin.

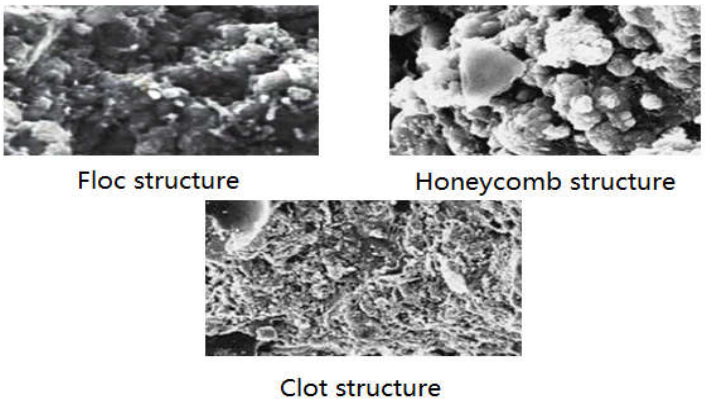

Figure 1. The microstructure of the sample soft soil

2.3. Effects of Soil Anisotropy

Soil anisotropy is mainly caused by two reasons: one is the structural reason, in the process of deposition and consolidation, the orientation of clay particles and their fabric units in natural soil layers results in soil anisotropy; the other is the stress reason, because the initial stress of natural soil layers is generally in an unequal stress state (the static earth pressure coefficient of normally consolidated soil is 0). Generally, it is not equal to 1, and the value of over-consolidated soil scale 0 is often greater than 1, which results in different increments of shear stress required for soil failure under different loading directions. In geological history, the natural soil layer is also affected by the surrounding environment (climate change, groundwater level rise and fall, historical glacial activity, etc.) and time. All these lead to the change of soil structure and initial stress state, which makes it more complex. Therefore, the anisotropy of soil becomes more complex. The anisotropy of soil can be measured by compression shear test of soil samples cut along different directions. The test results show that the strength of normal consolidated clay in horizontal direction is often less than that in vertical direction. From the sedimentary history of soil, the vertical direction is the main sedimentary direction of soil particles. The contact between particles is stronger than the horizontal direction after the vertical soil particles are compressed from top to bottom. Therefore, the shear strength in this direction is larger than the horizontal shear strength. There are two kinds of situations for the strength of soil samples in the direction of 45 degrees: the strength of some clay samples in the direction of 45 degrees is between the strength of horizontal soil samples and that of vertical soil samples (in most cases). The strength of some other clay in 45 degree direction is less than the strength of horizontal soil sample and also less than the strength of vertical soil sample.

2.4. Mohr-Coulomb Strength Theory Considering Porosity

For normal consolidated soils prepared in laboratory, the consolidation pressure in consolidated undrained shear test is recorded as σ_3, the axial stress in shear failure recorded as σ_1, the pore water pressure recorded as u, and the porosity recorded as n. Then, the maximum and minimum effective stresses considering the microstructure of soil can be derived as,

$$\sigma_1^{'} = \frac{B\sigma_1 - u}{B - 1} \tag{1a}$$

$$\sigma_3^{'} = \frac{B\sigma_3 - u}{B - 1} \tag{1b}$$

Where B is the pore pressure *is* coefficient. For saturated soils, the compressibility of water is much lower than that of soil skeleton, so it can be expressed as

$$B = \frac{1}{n^{\frac{2}{3}a}} \tag{2}$$

Where n is the soil porosity and a is a factor determined by the test. According to Mohr-Coulomb theory, the shear strength index of soil can be expressed as,

$$\tau_f = \sigma_c^{'} \tan\varphi^{'} \tag{3}$$

Where $\sigma_c^{'}$ represents the effective stress considering the micro-structure of soil, which is calculated by the effective stress circle considering the soil micro-structure.

3. Structural Calculation Model

3.1. Plane Pole System Finite Element Model

As FSPSs were arranged along a shoreline to form quay-walls, its longitudinal dimension was much larger than its transverse dimension. Thus, the guiding beam could be separated from framework to consider as a continuous beam structure, leaving piles and tensile truss partition simplified as a plane pole system model (Figure.2).

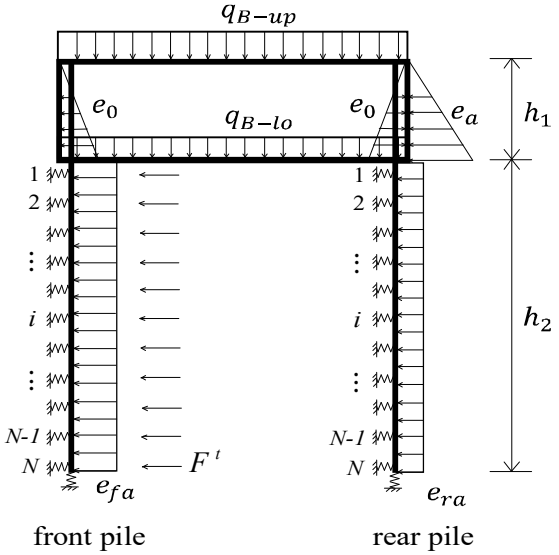

Figure 2. The plane pole system finite element model

Here piles, coupling beams and columns were modelled as elastic beam elements. Horizontal soil resistances on double-row piles were represented with two sets of level springs. A single vertical spring at pile tip was to simulate elastic support. Skin friction on pile was omitted since it mainly influenced axial force of pile rather than horizontal displacement, bending moment and shearing force along pile shaft. Alternative constraint types of rigid and articulated were adopted between pile and upper/lower coupling beam. The additional horizontal earth pressure was respectively applied on the back of both front and rear piles, and the vertical earth pressure load and service load were acted on the frame structure.

Stiffness coefficients of beam elements in unit width are listed in Table 1.

Table 1. Stiffness of beam elements (unit width)

Item	Pile	Coupling beam	Side-column	Mid-column
EI (kN·m^2)	2.47×10^5	2.95×10^5	1.72×10^6	1.51×10^5
EA (kN)	8.32×10^6	3.55×10^6	6.38×10^6	2.84×10^6

Plenty methods have been put forward to determine level subgrade reaction [16-19]. As horizontal displacement of pile is relatively small, m-method is suitable for calculating horizontal soil resistance. N nodes were placed along pile under framework, each node corresponding to a level spring, whose stiffness coefficient k_i was defined as,

$$k_i = K_i h_i = m_i Z_i h_i \tag{4}$$

Where K_i is the coefficient of level subgrade reaction at node i; h_i is height of soil layer corresponding to node i; m_i is a scale factor as K_i increasing with depth; Z_i is the distance from node *i* to framework bottom.

3.2. Load Calculating

Loads on cross beam of framework were supposed uniformly distributed. With sand backfilled inside framework and surcharges applied on the top surface of FSPS, loads on cross beam included soil gravity and surcharges of the part directly over the beam and the part at oblique upper position of beam on both sides, which transferred to the beam through soil interior friction. Beam loads were calculated by two methods, that respectively in way of skin friction (Figure.3 (a)) and vertical earth pressure diffusion (Figure.3 (b)).

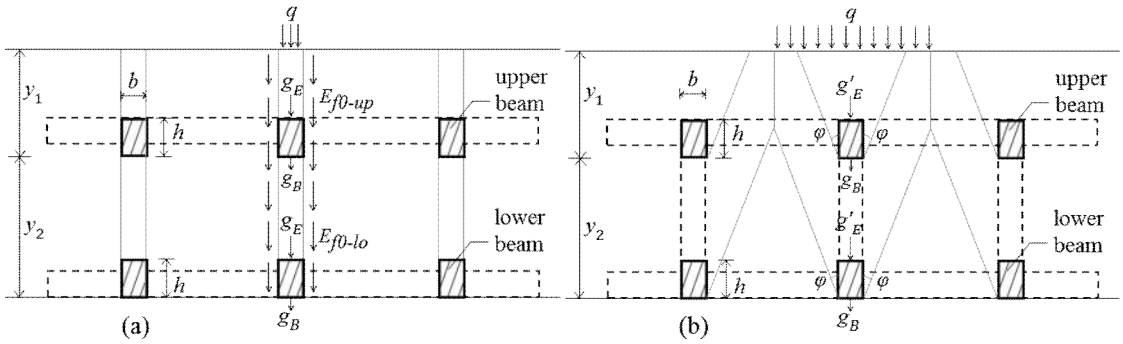

Figure 3. Illustration sketch of beam load calculation

The smaller result of above methods was chosen as the calculated load of beam, denoted as q_{B-up} and q_{B-lo} for the upper and the lower coupling beams respectively.

Due to large stiffness and small deformation of the frame structure, filling inside framework moved together with the framework under lateral load. Herein it was considered respectively as state earth pressure e_0 inside the framework and active earth pressure e_a behind the framework. Considering partial load applied on coupling beams, the additional active earth pressure on piles underneath the framework became smaller, namely

$$e_{fa} = K_a\left(\gamma_i h_1 + q - q_{B-up} - q_{B-lo}\right) + F^t \tag{5}$$

$$e_{ra} = K_a\left(\gamma_b h_1 + q\right) - e_{fa} \tag{6}$$

where K_a is the active earth pressure coefficient for subsoil; γ_i and γ_b are unit weight of filling inside and behind framework; h_1 is the distance from the top surface of structure to framework bottom; q is the distributed load on the top surface of structure; F^t is the migrating load introduced next.

3.3. Load Migrating from Rear Pile to Front Pile

As limited row spacing and low shearing resistance of subsoil, the interior soil was likely to fail in providing enough horizontal resistance for rear pile. Therefore, partial load would migrate from rear pile to front pile through the interior soil. This process was named as "load migration". Taking out the part of front plie, rear piles and interior soil between calculation plane *i* and frame structure from the whole section of structure, as shown in Figure.4.

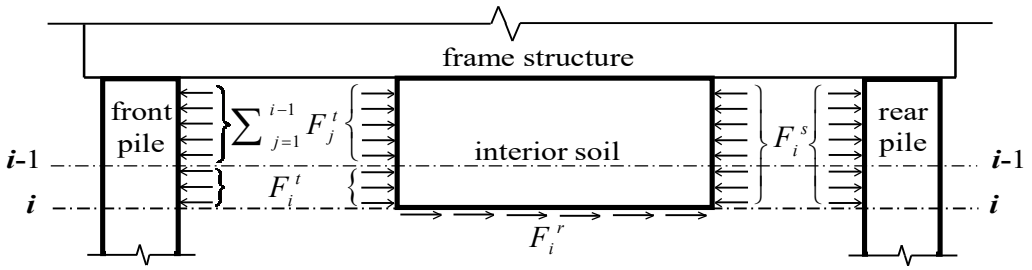

Figure 2. Analysis of "load migration" process

Total lateral force on interior soil above the calculation plane *i*, which caused by rear pile deformation, was

defined as

$$F_i^s = \sum_{j=1}^{i} k_{rj} x_{rj} \tag{7}$$

Where k_{rj} and x_{rj} are stiffness and horizontal displacement of spring on rear pile corresponding to node j.

The ultimate horizontal resistance provided by interior soil above calculation plane *i* was

$$F_i^r = \min\left\{E_{pi}, f_i\right\} \tag{8}$$

$$f_i = G_i \tan\varphi_i + c_i L \tag{9}$$

where E_{pi} is the passive earth pressure on rear pile produced by interior soil above calculation plane *i*; f_i is the sum of friction and cohesion generated on calculation plane *i*; G_i is gravity of interior soil above calculation plane i; *L* is row spacing; φ_i and c_i are internal friction angle and cohesive force of soil layer corresponding to calculation plane i.

The difference between total lateral force and ultimate horizontal resistance of interior soil migrated to front pile, defined as,

$$F_i^t = \begin{cases} \max\left\{0, F_i^s - F_i^r\right\}, & i = 1 \\ \max\left\{0,\ F_i^s - F_i^r - \sum_{j=1}^{i-1} F_j^t\right\}, & i = 2,3,\cdots,N \end{cases} \tag{10}$$

4. Analysis on Field Observations and Results of PPSFEM

4.1. Project observation

(1) Engineering structures and observations

The project in Tianjin Port, with a shoreline of 200m long, was composed of 12 groups of FSPS. The shear strength index *c* and *φ* in Table 2 were calculated according to Eq. (1)-(3), with consideration of clay soil micro-structure. M-values in Table 2 were determined by engineering geological condition and suggested values in the code.

Table 2. Properties of subsoil

No.	Layer	Depth (m)	γ (kN/m^3)	M-values(kN/m^4)	c(kPa)	φ(°)
–	Sand bag	6.0 ~ GL.	18.0	——	0	28.0
–	Rubble	6.0 ~ GL.	17.0	——	0	42.0
1	Mucky silty clay	GL. ~ -12.0	16.8	1000	10.0	0.7
2	Clay	~ -15.0	18.5	2500	27.3	7.9
3	Silty clay	~ -27.0	19.7	3000	17.9	14.1

As a test project of FSPS, the horizontal displacement of pile and vertical pressures of filling inside framework were measured under loading. Inclinometer tubes (Figure.5 (a)) and earth pressure cells (Figure.5 (b)) were used to measure horizontal displacement of pile and vertical pressures of filling inside framework.

Three rows of earth pressure cells (R1/R2/R3) were emplaced on the level datum plane of -0.5m (i.e. the upper surface of lower coupling beam). The character A, B and C stood separately for measuring points located at midpoints of cabins, nearby coupling beams and at coupling beams. It was backfilled inside and behind the framework respectively with sand bags and rubble to a design elevation of 6.0m. The structure was uniformly loaded to 23.4kPa firstly by heaping sand on wharf surface and loaded to 39.6kPa twenty days later. The measurement started when the backfilling began and continued until the second load was added and then was laid out for three months.

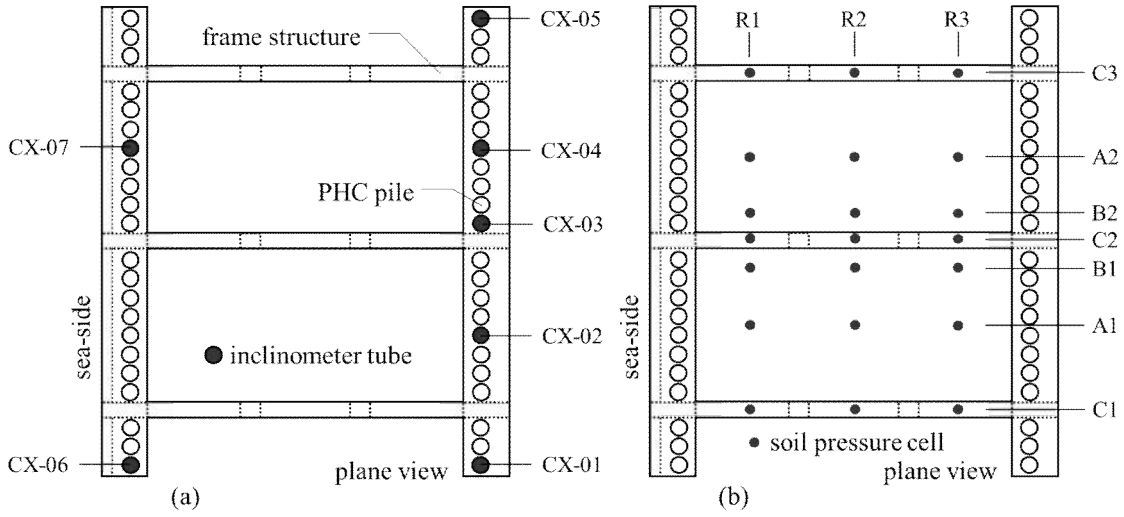

Figure 3. Location of measuring equipment

(2) Pile internal forces calculated by displacement curve

Bending moment and shearing force need to be derived from measured pile horizontal displacements for the lack of in-situ observation of pile internal forces. It is necessary to fit the displacement curve in advance by the least square method, since what obtained from field observation was just horizontal displacement of pile at a series of discrete points along pile shaft. The function of pile displacement $y(x)$ is supposed as $2n$+1 times Fourier series, that is,

$$y(x) = a_0 + \sum_{k=1}^{n} \left(a_k \cos k\omega x + b_k \sin k\omega x \right) \tag{11}$$

Where $\{\omega, a_0, a_k, b_k, k = 1,2,\cdots,n\}$ is a set of undetermined coefficients? Based on the discrete data of observed pile horizontal displacement $\{(x_i, y_i), i = 1,2,\cdots,m\}$, a function $y^*(x)$ can be obtained by the least square method. Herein the bending moment and shearing force distribution along pile shaft are derived by elastic beam theory, that is,

$$M(x) = EI \frac{d^2 y^*(x)}{dx^2} = -EI\omega^{*2} \sum_{k=1}^{n} k^2 \left(a_k^* \cos k\omega^* x + b_k^* \sin k\omega^* x \right) \tag{12}$$

$$Q(x) = \frac{dM(x)}{dx} = EI \frac{d^3 y^*(x)}{dx^3} = EI\omega^{*3} \sum_{k=1}^{n} k^3 \left(a_k^* \sin k\omega^* x - b_k^* \cos k\omega^* x \right) \tag{13}$$

4.2. Vertical Pressures of Soil inside Framework

A comparison of vertical pressures of soil inside framework under a load of 39.6kPa obtained from PPSFEM with that from field observations is shown in Table 3. The field-measured vertical earth pressure values are discrete in a large scope for the backfilling made up of sand bags rather than bulk sand. Thus, the average values of vertical earth pressure are calculated by removing those greatly deviated values italicized in Table 3.

Table 3. Comparison of vertical earth pressures inside framework (at -0.5m)

Locations	Field observations (kPa)									Average	Calculated result (kPa)	Relative deviation
Midpoints of cabins (A1/A2)	*30*	7	0	0	5	5				71.8	75.1	4.6%
Points nearby coupling beams (B1/B2)	6	8	*18*	0	8	*00*				65.5	75.1	14.7%
Points located at coupling beams (L1/L2/L3)	*5*	*0*	08	50	38	35	70	*1*	44	241	338.2	40.3%

In terms of vertical earth pressure at coupling beam, the average field data is 241kPa, whereas the theoretical calculation result is 143.5kPa by omitting influences of coupling beam. Obviously, the

coupling beam makes vertical earth pressure larger in comparison with the case without coupling beam, which is in agreement with the calculation thought of beam load proposed above. In terms of vertical earth pressure near*by* coupling beam, values obtained from theoretical calculation are apparently larger than that from field observation. Because the vertical earth pressure is supposed equal everywhere inside framework (except points on coupling beam) within identical elevation plane, and defined as the average of soil gravity minus the part applied on coupling beams. Actually, vertical earth pressure inside framework is not a uniform distribution because of coupling beams but increasing with distance away from the beam.

4.3. Horizontal Displacement of Pile

Horizontal displacement curves of piles obtained from PPSFEM with and without consideration of "load migration" are compared in Figure.6. Twice loadings are marked as "1" & "2", while "NLM" is short for "none load migration". It is indicated that the "load migration" process makes universal enlargement of horizontal displacement along pile shaft.

Horizontal displacement curves of piles obtained from PPSFEM are also compared with that from field observation (Figure.6).

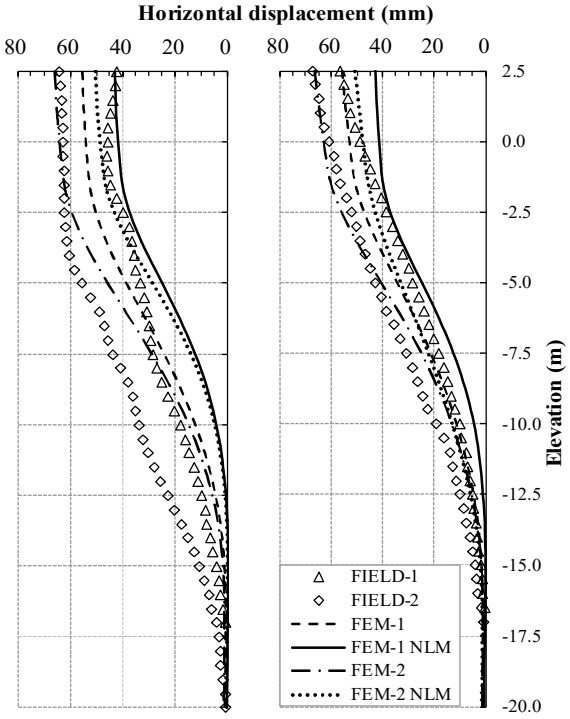

Figure 4. Comparison of pile horizontal displacement curves

The agreement between the different results of rear pile is very close. In terms of front pile, the maximum displacements are in close agreement, while PPSFEM result is clearly smaller than field observation of pile displacement at the range from -1.5m (i.e. framework bottom) to -15m.

Since piles are placed at a tiny internal, it can be considered as sheet-pile wall structure to calculate the soil resistance in terms of global stress analysis. Actually, soil resistance of soldier pile structure is less than the modelled result due to the large stiffness difference between pile and soil. Herein the measured maximum horizontal displacement at pile head is greater than result obtained from PPSFEM. Similar conclusion can be drawn respectively from observation and PPSFEM that displacement of front pile within the scope from 2.5m to -3m keeps consistency under the same loading, which contributes to confirm the restriction effect of frame structure on front pile deformation.

4.4. Bending Moment and Shearing Force of Pile

According to section 3.1.2, displacement curve of piles are fitted to calculate distribution of bending moment and shearing force along pile (denoted as "fitting results"). Comparisons of PPSFEM results with fitting results of front and rear pile are shown in Figure.7.

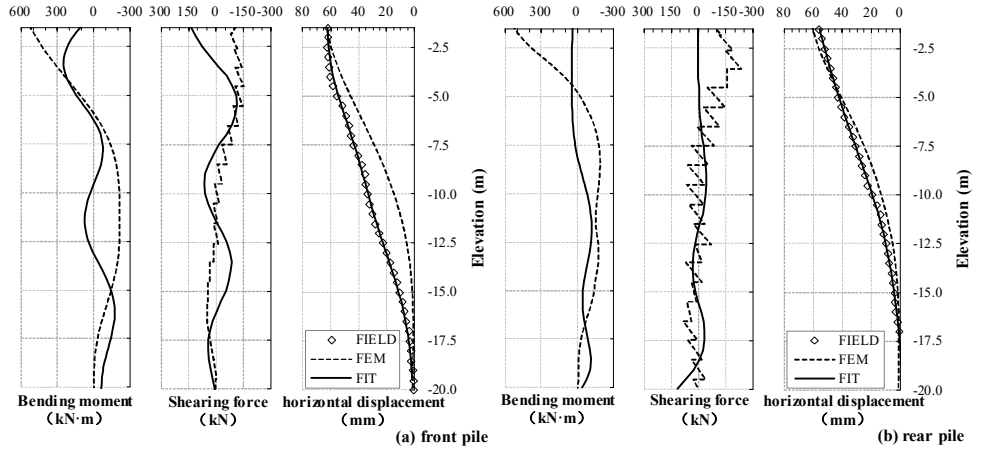

Figure 5. Internal forces and horizontal displacement (distributed loading of 39.6kPa).

The maximum bending moment and maximum shearing force obtained from PPSFEM are greater than that of fitting results, implying that results of PPSFEM are conservative and safe.

5. Analysis on Influence Factors of Pile Displacement and Internal Forces

5.1. Constraint Form between Pile and Under Part of Framework

Due to underwater construction, the quality of caulking concrete casted in the gap between lower guiding beam and piles is difficult to guarantee. Herein that concrete is likely to be broken under a large lateral load, resulting in conversion of constraint state between pile and underpart of framework from fixed one into articulated one. Distribution of horizontal displacement and internal forces along piles are obtained from two models with fixed and articulated constraint form (Figure.8).

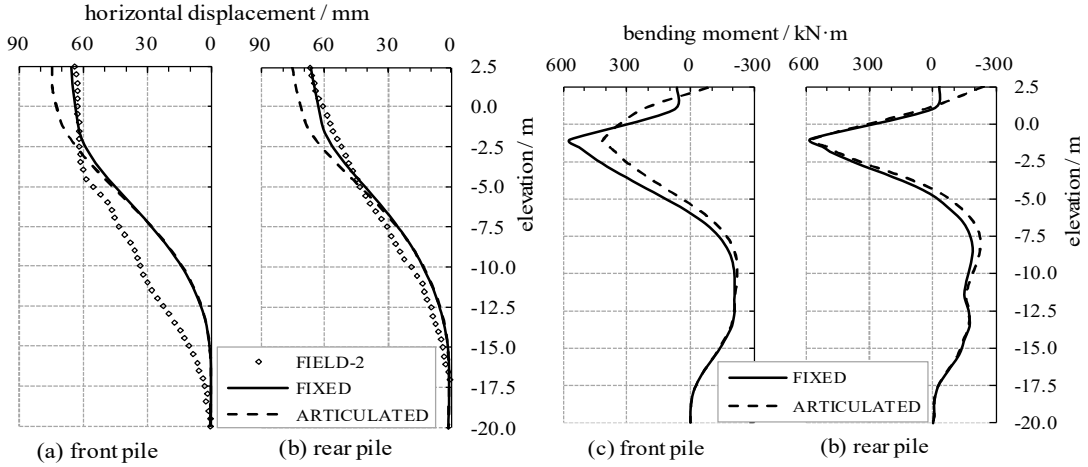

Figure 6. Effects of constraint form between beam and pile

The constraint form has an influence on horizontal displacement of pile body near the framework and little influence on that of pile body below -5m. Comparing with fixed constraint, the articulated one increases maximum displacement and decreases maximum bending moment by 30 percent for front pile, but impacts barely on bending moment of rear pile. If the displacement permits, adopting the articulated constraint form between pile and underpart of framework is helpful to control pile internal forces.

5.2. M-values of Subsoil

Level subgrade reaction is determined by m-values of subsoil, which affects distribution of pile displacement and internal forces. Due to the feature of separated piles and stiffness difference between soldier pile and adjacent soil, soil resistance on soldier pile structure is less than that on sheet-pile wall structure, which can be simulated by reducing m-values. Results obtained by PPSFEM with m-values modified by multiplying factor α (α=0.3, 0.5, 1.0 &1.5) are shown in Figure.9.

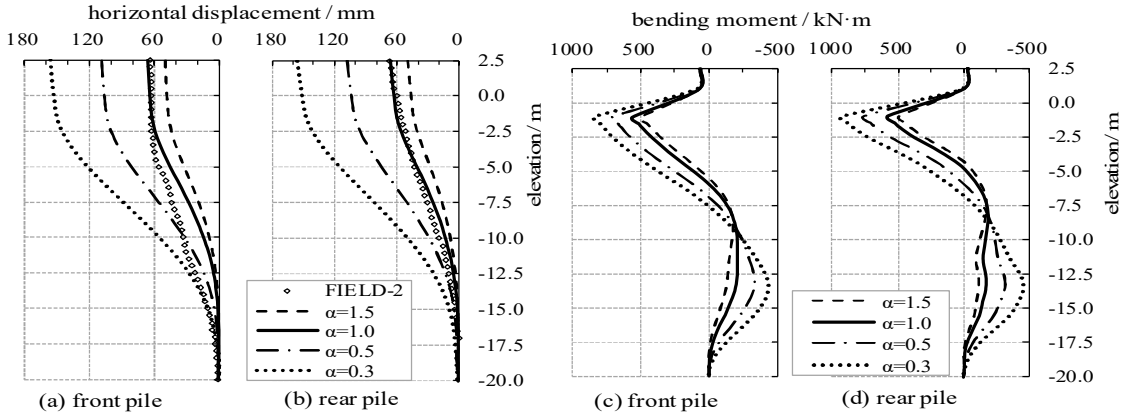

Figure 7. Effects of m-values of subsoil

The horizontal displacement and bending moment increase rapidly with α decreasing. Compared with α=1.0, the agreement between horizontal displacements obtained from PPSFEM and field observation is closer as α=0.5, though the difference between maximum displacement of calculated results and measured data is considerable. In fact, considering varied stiffness of subsoil, the stiffness ratio of pile and soil changes along pile shaft. It is not suitable to reducing m-values of different soil layer by identical factor, and further study is needed on α changing with stiffness ratio.

5.3. Backfilling Materials Inside and Behind the Framework

Four combination schemes of backfilling materials inside and behind the framework (Table 4) are discussed here to study their effects on pile displacement and internal forces.

Table 4. Combination schemes of backfilling materials

Combination schemes	1	2	3	4
Inside framework	sand	sand	dredger fill	dredger fill
Behind framework	stone	dredger fill	stone	dredger fill

Results obtained from PPSFEM are illustrated in Figure.10.

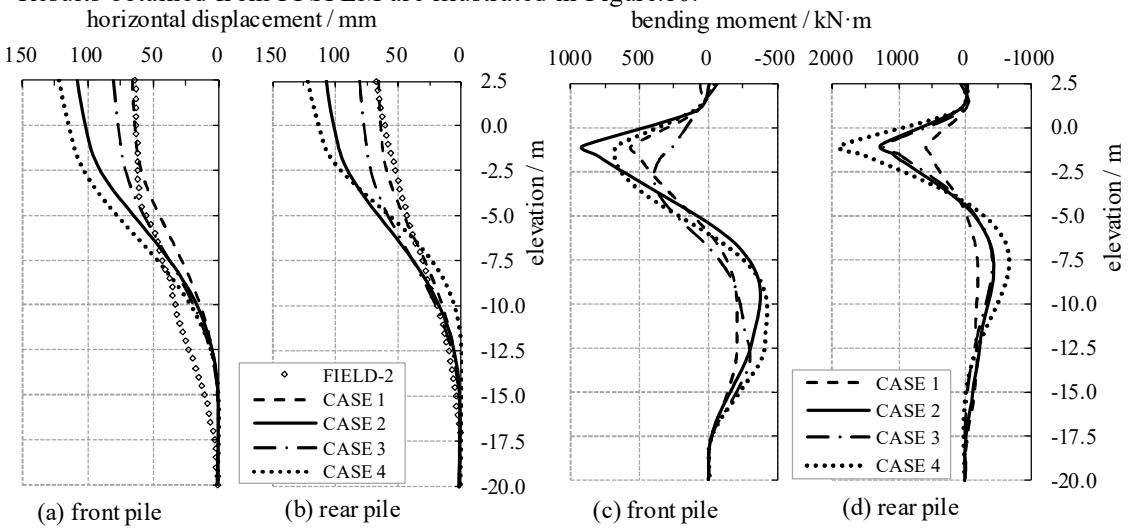

Figure 8. Effects of backfilling materials

In terms of backfilling material inside the frame structure, as the case of dredger fill compared with the case of sand, maximum horizontal displacement of both front and rear piles enlarge by 14% ~ 22%, bending moment of front pile reduces while that of rear pile increases. As most gravity of dredger fill applied on the subsoil due to smaller values of φ, the additional active earth pressure applied on front pile becomes larger, which gives rise to the increase in axial forces of coupling beams and internal forces

of rear pile?

Backfilling material behind framework has significant effects on pile horizontal displacement. As stone is replaced by dredger fill behind the framework, the maximum displacement of pile head increases by 52% ~ 63%, the maximum bending moment increases by 61% ~ 72% for front pile and increases by 47% ~ 120% for rear pile. If conditions permit, sand and stone are better choices for backfilling to reduce displacement and bending moment of pile.

6. Conclusions

PWFS is a new type of double row pile fence structure, which has the characteristics of small pile spacing and large row spacing. When it bears horizontal load, the front row pile bears the main load. Considering that the macroscopic physical and mechanical properties of soil are affected to some extent by the state and change of micro-structure, the relationship between micro-parameters and macro-physical quantities of soft clay is established by statistical method based on the SEM test of soft clay.

(1) In term of stress and deformation of FSPS, a PPSFEM can by employed to solve the distribution of horizontal displacement and internal forces along pile under lateral load. The frame structure and piles were modelled as elastic beam elements. Based on subgrade reaction approach, horizontal soil resistances on piles were represented with level springs whose stiffness coefficients were determined by "m" method. Interior soil was treated as ideal elastic-plastic material. The process of "load migration" was considered. Namely, partial load would transfer from rear pile to front pile via interior soil, as a level thrust applied on interior soil is larger than the ultimate resistance. According to engineering parameters of a test project, horizontal displacement of pile and vertical pressures of soil inside framework were obtained from PPSFEM. Agreement between results drawn from model and data obtained from the test project is very close, which verifies the feasibility of the proposed calculation model.

(2) The upper frame structure can support part of vertical load and filling gravity to reduce the additional vertical earth pressure of subsoil at the bottom of framework. The upper frame structure can restricts pile deformation to improve the internal force distribution of pile foundation. It is beneficial to reduce the maximum bending moment of pile by adopting articulated constraint form between pile and underpart of framework.

(3) Unit soil resistance on front pile becomes smaller due to the feature of separated piles, which can be simulated in the calculation model by reducing "m-values". Further study is still needed on the specific reduction rules. Sand and stone are better choices for backfilling both inside and behind the framework to reduce displacement and internal forces of pile.

References

[1] Hui Z. (2011) "Microscopic Mechanism Study on Engineering Properties of Soft Soil in Pearl River Delta", *Industrial Construction*, 41(7), pp. 82-86.

[2] Liang, S. H, Zhou, S. Z. (2015) "Experimental Research about Mechanical Properties and Microscopic Structures of Nansha Soft Soil Stabilised with Slag and Cement", *Materials Research Innovations*, 19(sup10), pp. S10-69.

[3] Tang, Y. Q, Yan, J. J. (2015) "Effect of Freeze–Thaw on Hydraulic Conductivity and Microstructure of Soft Soil in Shanghai Area", *Environmental Earth Sciences*, 73(11), pp. 7679-7690.

[4] Wang, J., Mo, H. H., Liu, S. Z. (2014) "Effect of Mineral Composition on Macroscopic and Microscopic Consolidation Properties of Soft Soil", *Soil Mechanics & Foundation Engineering*, 50(6), pp. 232-237.

[5] Zheng, G., Li, X., Liu, C., Gao, X. (2004) "Analysis of Double-row Piles in Consideration of the Pile-soil Interaction", *Journal of Building Structures*, 25(1), pp. 99-106. (in Chinese)

[6] Yu, L. X., Zhou, G. R. (2004) "Study on a New Type of Double Row Pile Wharf Structure", *Technology and Management of Port Engineering,* 1, pp. 1-6. (in Chinese)

[7] Chen, L.T., Poulos, H.G., Hull, T. S. (1997) "Model Tests on Pile Groups Subjected to Lateral Soil Movement", *Soils & Foundation,* 37(1), pp. 1-12.

[8] Chow, Y.K. (1996) "Analysis of Piles Used for Slope Stabilization", *Int J Numer Anal Met.* 20(9), pp. 635-646.

[9] Pan, J. L., Goh, A. T. C., Wong, K. S., Teh, C. I. (2002) "Ultimate Soil Pressures for Piles Subjected to Lateral Soil Movements", J Geotech Geoenviron, 128(6), pp. 530-535.

[10] Guo, W. D. (2014) "Elastic Models for Nonlinear Response of Rigid Passive Piles", *Int J Numer Anal Met.* 38(18), pp. 1969-1989.

[11] Chen, J., Feng, Y., & Shu, W. (2016) "An Improved Solution for Beam on Elastic Foundation Using Quintic Displacement Functions", *KSCE Journal of Civil Engineering*, 20(2), pp. 792-802.

[12] Kim, B.T., Yoon, G. L. (2011) "Laboratory Modeling of Laterally Loaded Pile Groups in Sand", *KSCE Journal of Civil Engineerin,* 15(1), pp. 65-75.

[13] Rollins, K. M., Lane, J. D., Gerber, T. M. (2005) "Measured and Computed Lateral Response of a Pile Group in Sand", *Journal of Geotechnical and Geoenvironmental Engineering,* 131(1), pp. 103-114.
[14] Cai, F., & Ugai, K. (2011) "A Subgrade Reaction Solution for Piles to Stabilize Landslides", *Géotechnique*, 61(2), pp. 143-151.
[15] Hsiung, Y. M. (2003) "Theoretical elastic-plastic solution for laterally loaded piles", *Journal of Geotechnical and Geoenvironmental Engineering*, 129(5), pp. 475-480.
[16] Hu, L., Liu, X. (1998) "An Iteration Method for Computation of Flexible Fender Piles", China Ocean Engineering, 12(4), pp. 435-442.
[17] Jin, W., Zhu, Y., Li, L. (1993) "Evaluation of Application of P-Y Curve Method in Offshore Engineering Foundation", China Ocean Engineering, 7(4), pp. 451-466.
[18] Ziai, L. (1997) "Modulus of Subgrade Reaction for Laterally Loaded Piles in Multiple Layered Foundation", China Ocean Engineering, 11(4), pp. 477-486.
[19] Liu, T., Chen, Y. B. (2013) "The Safety Assessment of Bored Pile Retaining Wall Based on Back Analysis for Bending Moment", *Applied Mechanics & Materials,* 353-356, pp. 1015-1023.